JOURNAL OF MATERIALS SCIENCE **39** (2004) 6561–6569

Mechanical properties and microstructural characterization of extrusion welds in AA6082-T4

A. LOUKUS, G. SUBHASH*, M. IMANINEJAD
Mechanical Engineering-Engineering Mechanics Department, Michigan Technological University, Houghton, Michigan
E-mail: subhash@mtu.edu

Microstructural observations of extrusion welds in an A-pillar made of AA6082-T4 revealed that the observed extrusion weld is a composite of a seam weld (longitudinal weld) and a charge weld (transverse weld). To determine the mechanical properties of this weld region, tensile specimens were prepared with the weld located at 0°, 45°, and 90° to the tensile axis. For comparison purposes, specimens from no-weld regions were also prepared in the same orientations and tested. The specimens with 45°-weld exhibited the lowest tensile strength, followed by the specimens with 90°-weld, no-weld and 0°-weld specimens. Comparison of failure strains and fracture modes revealed that weld regions are less ductile than the no-weld regions. Microscopic observations of fractured surfaces and further analysis revealed that Mg_2Si precipitates that align along the charge weld cause premature failure at these locations.

1. Introduction

Extrusion welds are an inevitable consequence of the extrusion process. These welds are present in both closed-loop and some open-loop cross sections. When a heated aluminum billet is pushed into an extrusion die cavity, the material flows around the mandrel supports and is welded in the solid state, as shown in Fig. 1, to form extrusion welds. Extrusion welds, as they are broadly termed, consist of a seam weld (longitudinal weld) and a charge weld (transverse weld) [1, 2]. Seam welds are formed as material streams around the mandrel supports in a porthole die and are brought into intimate contact in the welding chamber [1]. In the industrial extrusion facilities, several billets may be extruded in succession. After an extrusion cycle, some material from the previous billet remains in the extrusion die ports even after the back end of the billet is cut off. During the next cycle, the following billet pushes the material from the previous billet through the extrusion die (see Fig. 2). The resulting solid state welding between these two billet materials forms "tongue" shaped "charge welds", also called transverse weld. Although the extrusion welds form a small fraction of the overall volume of any extruded shape, they are sometimes responsible for premature failure of a finished part during a forming operation [1]. This is because failure often occurs at or near these welds thus limiting the capability of the material to achieve more complex shapes during forming processes. Understanding the influence of extrusion welds on the overall mechanical behavior of a component is essential because the extrusion welds are known to affect formability, failure location, fatigue life, and strength of extruded parts in service [1–3]. This knowledge can assist in positioning mandrel supports in the porthole dies thus controlling the locations of the extrusion welds in an extruded part. Product design engineers can utilize such information on extrusion welds to assess whether a specific complex feature can be formed based on the forming limits of the weld and no-weld regions. Die designers can also employ this information to avoid premature part failures at a specific location during service. By locating weld-affected regions away from high stressed regions of the part to be formed, they can probably enhance the overall formability of some alloys.

To illustrate the motivation for the current study, a typical failure pattern of a hydroformed tube of AA6082-T4 is shown in Fig. 3, where the seam weld location is indicated by a dark line. Analysis of several experiments performed by the authors also revealed that failure does not occur exactly on the seam weld line but occurs in the close proximity [3]. Thus, extrusion welds could play a significant role in the formability of aluminum tubes since the failure location is consistently adjacent to a weld. Therefore, the resulting formability is for the composite material consisting of weld and no-weld regions of an extruded tube. Since extrusion welds are unavoidable in many extruded parts (due to economical and manufacturing reasons), investigating their effect on formability and failure of the material is of considerable practical importance and is industrially relevant. The additional ductility inherent in the no-weld regions needs to be quantified (in the absence

*Author to whom all correspondence should be addressed.

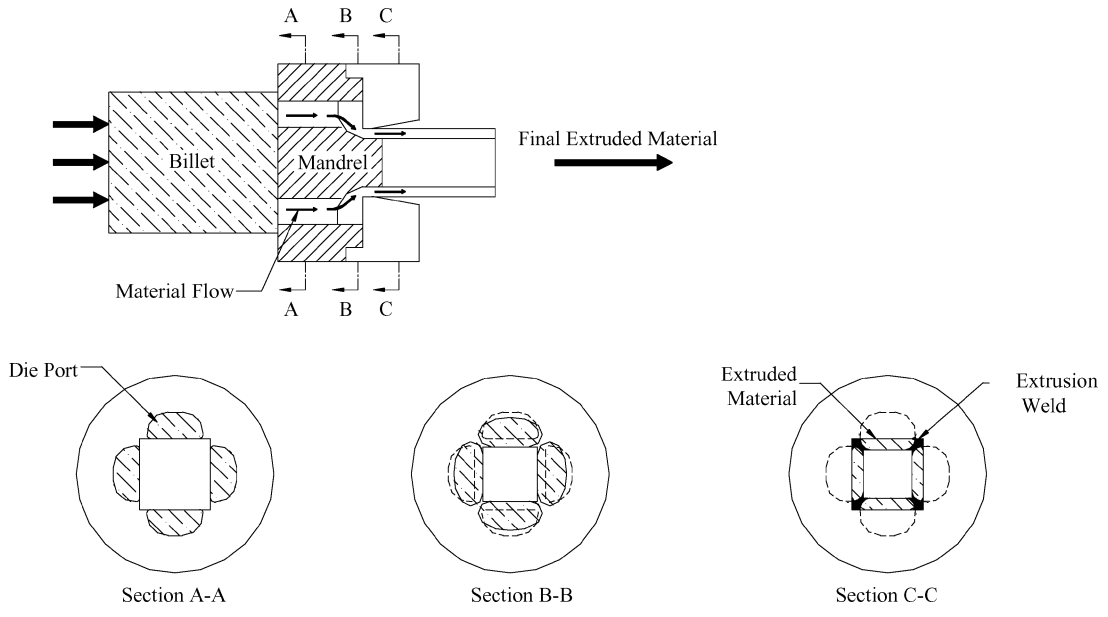

Figure 1 Schematic of extrusion process illustrating the formation of extrusion welds in a tube.

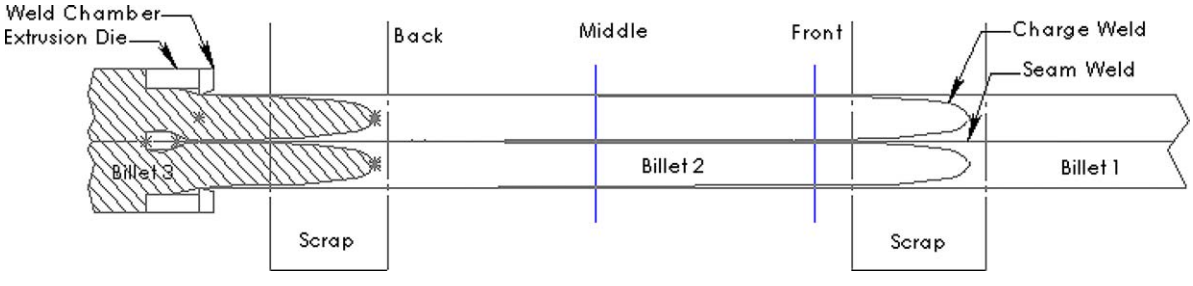

Figure 2 The extrusion welding process showing the seam weld and charge weld. Scrapped material and the locations from which specimens are taken are indicated.

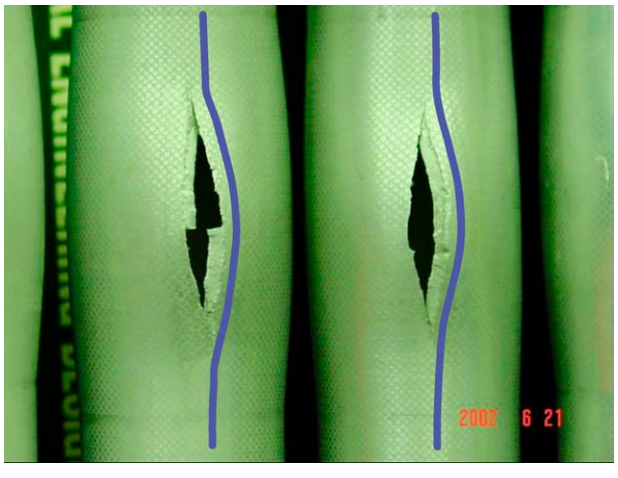

Figure 3 Failure of AA6082-T4 tubes close to the seam weld (indicated by dark line) during hydroforming.

of welds) in order to realize the full potential of the material.

Although extrusion welds play a critical role in premature failure of the studied material, they may not affect the failure characteristics in some other alloys [2, 3]. Further studies by the authors revealed that in AA6063-T4, the welds play an insignificant role in the failure patterns of the material.

Many laboratory studies on formation and characterization of extrusion welds are available but the literature on the influence of "industrially produced" extrusion welds is limited. Most of the pioneering works on the macroscopic and microstructural elements involved in extrusion welds in aluminum alloys, formation process of these welds and material flow in complex extrusion dies were performed by Akeret [1]. He concluded that the weakest link of the extrusion weld is the charge weld regions and cautioned to avoid lubricants on billet faces that will contaminate charge welds. Material flow in extrusion dies and the solid state bonding immediately after the mandrel supports were well investigated in specially made laboratory dies by Valberg [2]. He also performed extensive work on defects in extrusion welds and the factors responsible for their initiation by innovatively placing lines of marker material in billets prior to extrusion. He also illustrated material flow in the extrusion container as well as in the extrusion die using emptying diagrams [2]. Such studies assisted in understanding dead metal zones and shear interfaces around mandrel supports. Gjerstad [4] investigated flow of material in the weld chamber and the resultant weld fatigue strength. For given extrusion parameters, different geometries of bridges (mandrel supports) resulted in different flow of the material. Based on results obtained from tensile and rotating bend tests, he proposed an optimal bridge geometry that can produce a weld with the highest strength and the best fatigue properties. Zasadzinski *et al*. [5] designed and fabricated extrusion

dies to investigate the influence of extrusion parameters in producing an extrusion weld. Uni-axial tensile tests performed along the extrusion length indicated that the position of the extrusion weld (i.e., distance from edge of the billet) did not affect the mechanical properties. However, if the fracture occurred outside the weld region, it was concluded that the extrusion parameters were in a manner that the weld was created successfully. Fracture occurring within the weld region, led to the conclusion that the parameters were not optimized to guarantee a good quality extrusion weld. Based on these experiments, Zasadzinski *et al*. [5] defined optimal parameters to obtain good quality extrusion welds. Although the above experiments were well conducted, since, the material was not in the heat-treated condition (T4 or T6) the influence extrusion welds was deemed minimal in the forming process [3].

The current research focuses on microstructural characterization and mechanical property determination of the extrusion welds at different weld orientations from a commercially extruded, heat-treated, aluminum alloy. Tensile properties and ductility of the weld-affected and no-weld regions were compared and analyzed.

2. Specimen preparation and experimental procedure

Extruded "A-pillar" frames of aluminum alloy 6082-T4 were obtained from Hydro Aluminum Technology Center, N.A., Holland, Michigan. To identify the location of welds on the A-pillar cross section, a small piece was cut out from the extrusion cross-section and was ground with 240, 320, 400 and 600 grit abrasives successively. The entire surface was then polished with a 6 mm diamond paste and etched initially with a 25% NaOH + 75% water solution to locate the weld regions. These regions were further etched with heated (∼60°C) NaOH solution for an additional two minutes. Observations under a stereomicroscope revealed the weld regions with greater contrast. Micrographs presented in Figs 4 and 5 illustrate the A-pillar cross-section and the weld-affected microstructure. It is clear that each extrusion weld consists of two distinct zones; a central seam weld line, surrounded by material from the previous billet, shown in Fig. 2. This material is charge welded to the new billet material on the "tongue shaped" boundary [1].

Optical micrographs of this region, shown in Fig. 5a and b, reveal that there is a distinct change in grain size and surface topography on opposite sides of this charge weld interface. Scanning electron microscope (SEM) observation of this interface between the new billet material and the previous billet material revealed aligned precipitates along the weld boundary as seen in Fig. 5c and d. Also, note that precipitates do exist on both sides of this charge weld, but are randomly distributed. More discussions on the formation of precipitates and their influence will be presented later in this paper.

The A-pillar cross-section was ideally suited for investigation of mechanical properties of welds because it contained one extrusion weld in the flat section (see

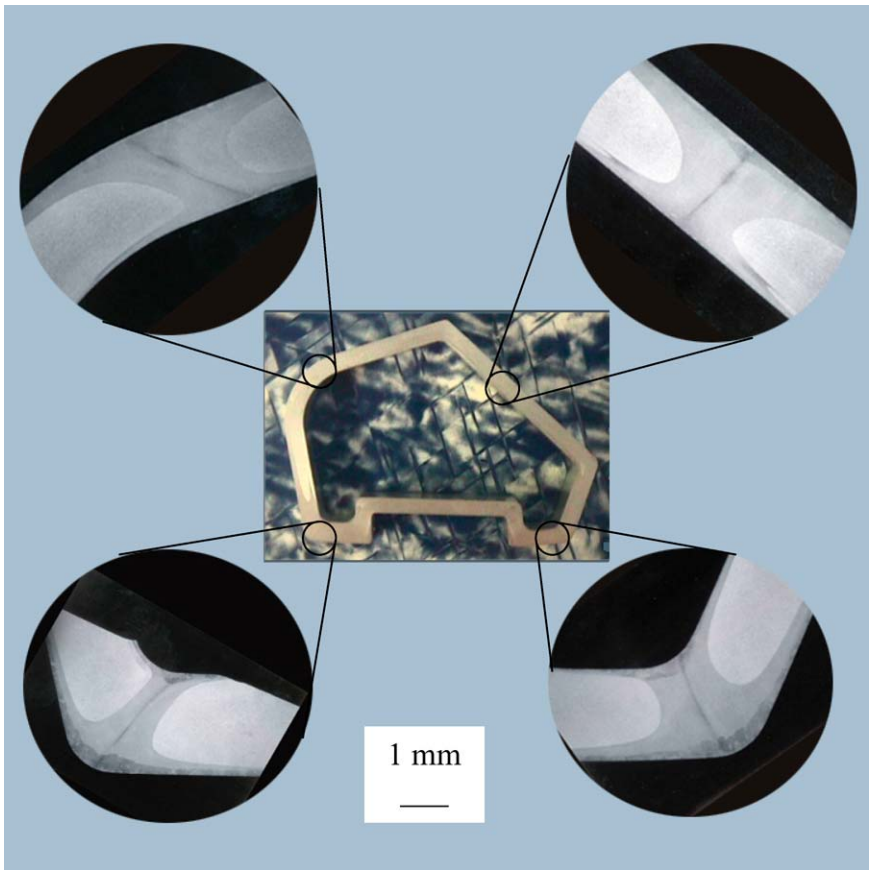

Figure 4 Micrographs of polished and etched A-pillar cross-section revealing the weld regions.

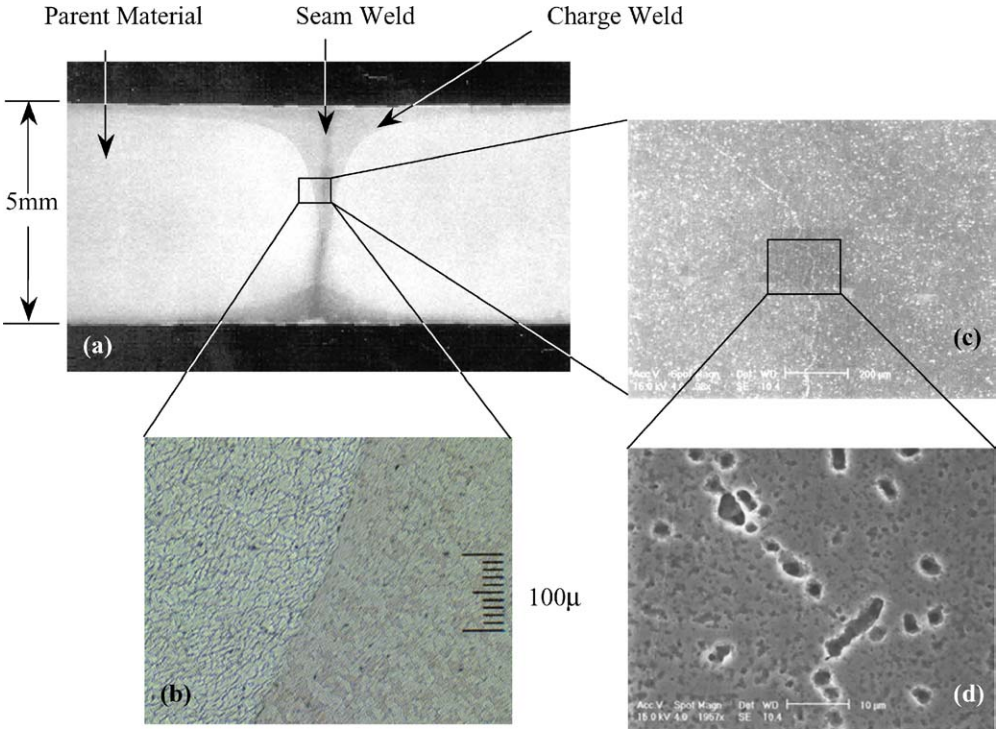

Figure 5 (a) Detailed view of the weld-region, (b) optical and (c) scanning electron micrographs of the weld boundary, and (d) aligned precipitates along the weld boundary.

Fig. 4) from which tensile samples could be obtained. It also contained a flat region with no extrusion weld (for comparison purposes). However, due to the limited width of the available flat side, precise ASTM B557 tensile specimens could not be cut from the frames. Thus, the dimensions were proportionately reduced to conform to the standards. Using a water jet machine, tensile specimens containing the above extrusion weld were cut at 0°, 45° and 90° to the weld line, as shown in Fig. 6a. For comparison purposes, specimens were also prepared from no-weld regions at similar orientations. It is important to realize that the position of the tensile specimens taken from extrudate plays an important role in that specimen's mechanical properties [3, 5]. This is because material elements throughout the cross section experience different shear and varying strain rates during the extrusion process. Specimens without weld (called 'no-weld' specimens) were taken from the bottom flat section (Fig. 6a). Typical tensile specimen dimensions are provided in Fig. 6b.

To fully capture the influence of the weld on material properties, the first set of tensile specimens were cut with the extrusion weld fully enclosed in the gage section. Since the weld forms only a small fraction of the overall material volume in the gage section, for 0° specimens the gage width was successively reduced

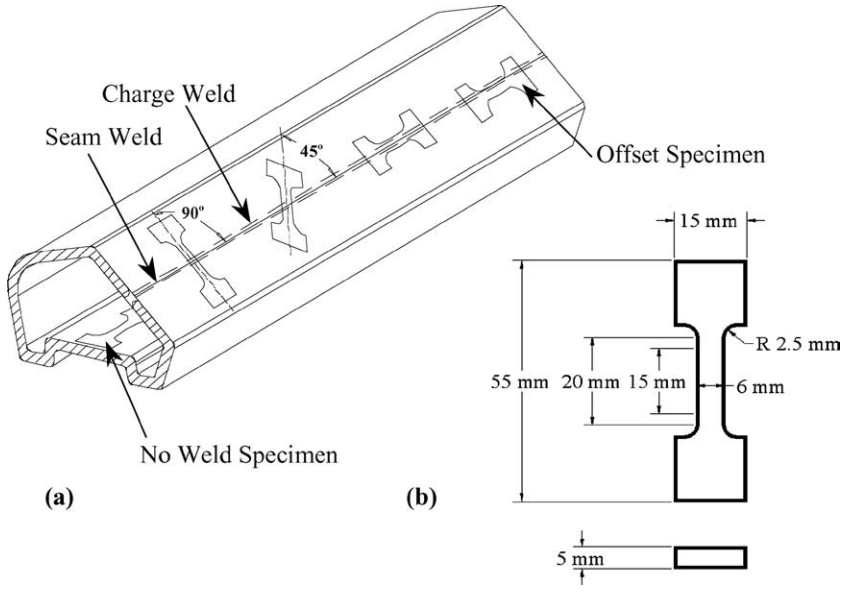

Figure 6 (a) Orientations of tensile specimens cut from an A-frame cross-section and (b) schematic of the tensile specimen dimensions.

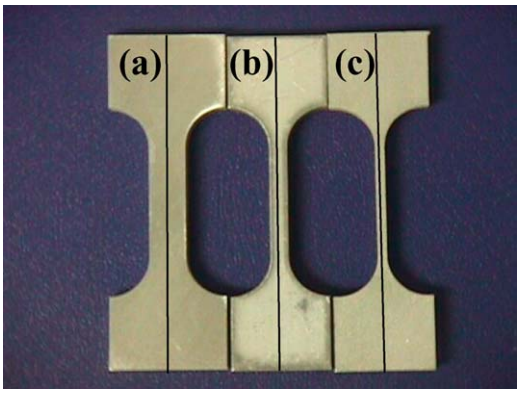

Figure 7 Tensile specimens with increasing fraction of weld material in the gage section. Gage width (a) 6 mm, (b) 3 mm, and (c) 1.5 mm.

from 6 to 3 mm and finally to 1.5 mm, as shown in Fig. 7, keeping all other dimensions constant. These successive reductions allowed the extrusion weld material volume to be a greater fraction of the total material volume of the gage section, thus allowing for investigation of the weld influence on tensile properties. The thickness of tensile specimens was held constant at 5 mm. Since failure in hydroforming experiments does not occur exactly on the seam weld, but occurs in the adjacent charge weld region (see Fig. 3), tensile specimens were also made parallel to the seam weld, with only charge weld regions in the gage volume. These are called "offset" specimens (see Fig. 6) in the subsequent plots and discussions. With the weld location clearly marked on the specimens, uni-axial tensile tests were performed at room temperature using an Instron testing machine. The crosshead speed for all performed tests was kept constant at 5 mm per minute.

3. Experimental results

3.1. Influence of orientation

Figs 8–10 illustrate the effect of the weld orientation on yield strength, ultimate tensile strength (UTS) and failure strain, respectively, for the specimen with gage width of 3 mm. The data from 3 mm samples were used because they were able to capture the extrusion weld region without excess parent material. These figures also show the results of the no-weld specimens obtained at similar angles to the extrusion weld direction and the

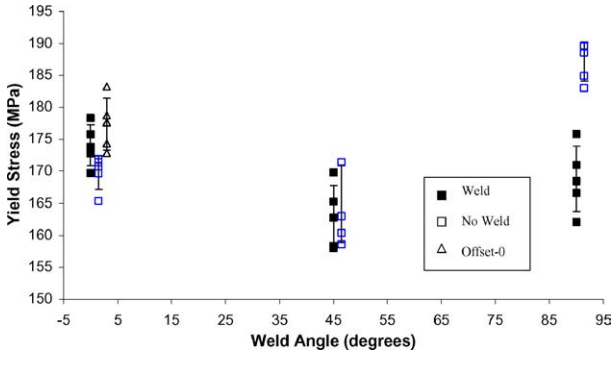

Figure 8 Comparison of yield stress of the specimens with weld, with no-weld and with offset to the weld at three orientations to the extrusion direction (gage dimension: 3 mm × 5 mm).

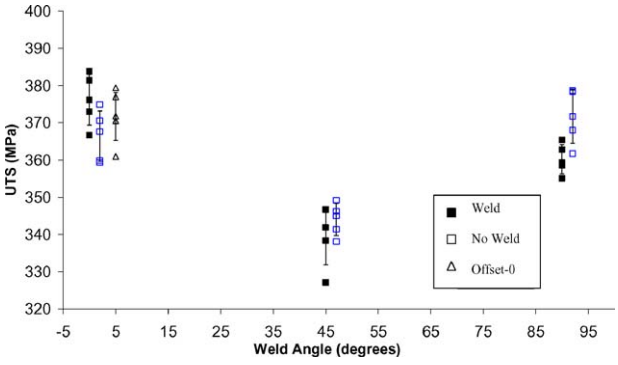

Figure 9 Comparison of UTS of the specimens with weld, with no-weld and offset to the weld at three orientations to the extrusion direction (gage dimension: 3 mm × 5 mm).

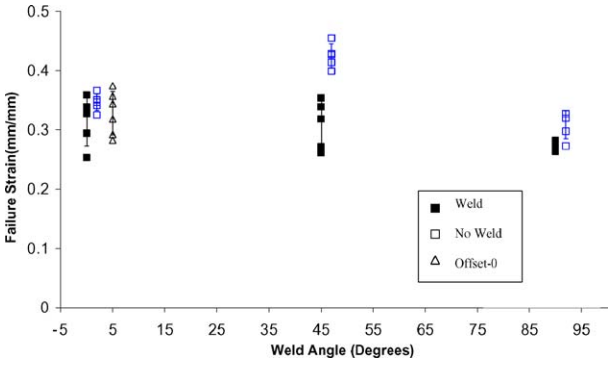

Figure 10 Comparison of failure strain of specimens with weld oriented at different angles to the tensile axis (gage dimensions: 3 mm × 5 mm).

results of the weld-offset specimens at 0°. From Figs 8 and 9 the following conclusions can be drawn: (i) The yield stress and the UTS of the weld and no-weld specimens is almost the same in 0° and 45° orientations. (ii) Slightly lower UTS and a 10% decrease in yield stress is noticed in the weld specimens when the weld is at 90° to the tensile axis. (iii) The orientation of the specimen to the extrusion direction has a more significant influence on the UTS compared to the existence of the weld in that direction. The yield strength is affected more by a weld at 90° to the tensile axis than its orientation to the extrusion direction. (iv) In general, higher yield strength and UTS occur when the weld is oriented along the tensile axis or the extrusion direction (i.e., 0° direction), and the lowest yield strength and UTS occurred when the weld was oriented at 45° to the tensile axis.

The failure strain, shown in Fig. 10, revealed a different trend than the UTS and yield strength. (i) The tensile specimens in all three orientations exhibited almost the same failure strains. (ii) At 0° to the tensile axis, strain to failure is the same in no-weld, weld and offset specimens. (iii) For weld specimens oriented at 45° to the tensile axis, the strain to failure is almost 25% smaller than that of the specimen with no-weld.

3.2. Influence of gage width

From the previous results, it is clear that the specimens with 0° weld orientation had almost the same yield strength, UTS and failure strain as the no-weld

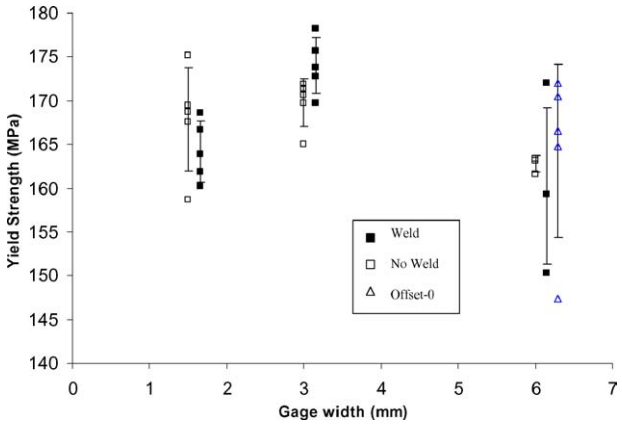

Figure 11 Influence of gage width on yield strength for 0°-weld specimens.

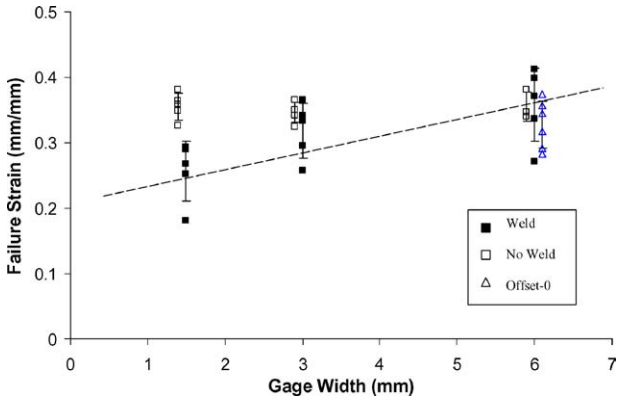

Figure 13 Influence of gage width on strain to failure for 0°-weld specimens.

specimens in this orientation. The tensile specimens with welds at 0° to the tensile axis were chosen to verify if the weld volume fraction within the gage section affects mechanical properties. As discussed earlier, the gage width was successively reduced by half (see Fig. 7) thus increasing each time the volume percentage of extrusion weld in the gage section. Note that in the other two orientations, the weld volume fraction cannot be changed unless the gage length is also reduced to the same size as the weld width.

Fig. 11 shows the yield strengths of these tensile specimens with different gage widths. The results do not show a significant trend. The experimental data shows that the yield strength values are unaffected by the extrusion weld volume fraction in the gage section. However, the scatter in the yield stress values appears to be greater in specimens with 6 mm gage width.

Fig. 12 illustrates the influence of the weld volume fraction (or gage width) on the UTS. When the gage width is reduced to 1.5 mm (or the weld material volume fraction is increased) the weld-specimens revealed a lower strength compared to the no-weld material. In addition, the scatter in the data increases with increasing weld volume fraction. For comparison purposes, the UTS data of the no-weld specimens (parent material), and the 6 mm "offset" specimens, are also shown in this figure. It is once again noticed that the difference in the UTS values diminishes with increasing gage width.

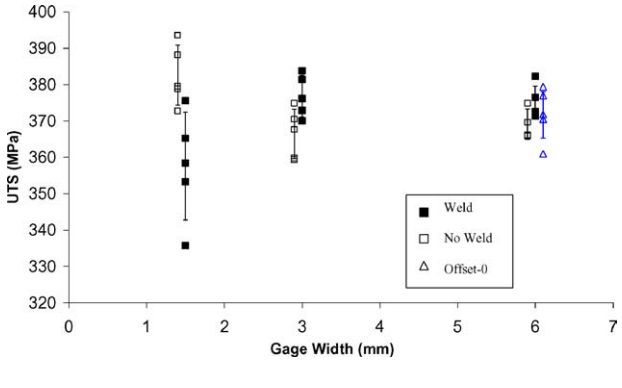

Figure 12 Influence of gage width on UTS for 0°-weld specimens.

The strain to failure data for the above specimens is summarized in Fig. 13. Compared to the UTS data, the failure strains were less scattered and revealed a moderately decreasing trend as the gage width decreased. The 1.5 mm specimens showed almost a 30% reduction in the strain to failure compared to the specimens with 6 mm width. This result along with the previous UTS data demonstrated that the weld material is less ductile than the parent material with no-weld.

3.3. Characterization of fracture surfaces

Fig. 14 illustrates the fracture modes in all the specimens with 3 mm × 5 mm gage section. Since the failure patterns of no-weld specimens are similar to those of the 0° weld specimens, these fracture specimens are not shown here. From the figure, it is evident that the orientations of the fracture plane to the tensile axis, as well as its fracture morphology are strongly a function of the weld orientation. When there is no weld (not shown) or when the weld is at 0° to the tensile axis, the fracture plane is smooth and is similar to typical ductile fracture at approximately 45° to the loading axis as shown in Fig. 14a. However, the specimens with 90°-weld orientation (Fig. 14c) fractured in a plane apparently parallel to the weld interface. A closer look at the typical fracture surfaces, shown at the right of each set of specimens, revealed that the no-weld specimens, showed a smooth ductile fracture plane but the 45° and the 90°-weld specimens revealed multiple fracture planes, uncharacteristic of typical ductile fracture. It should be noted that in these two later sets of specimens the fracture did not occur along the central weld line but slightly away from the weld (see Fig. 14b and c). These results suggest that the region surrounding the central weld line, i.e., the weld-affected (charge weld) region (see Fig. 5a) is primarily responsible for fracture during the uni-axial tensile tests.

In Fig. 15, the fracture surface of 0°-weld specimens with various widths are presented. Once again, note that as the gage width is reduced (or the weld material volume fraction is increased) the fracture occurs on multiple planes, indication of typical brittle fracture. Further microscopic investigations and analyses were conducted to identify the causes for such fracture patterns and are discussed in the following section.

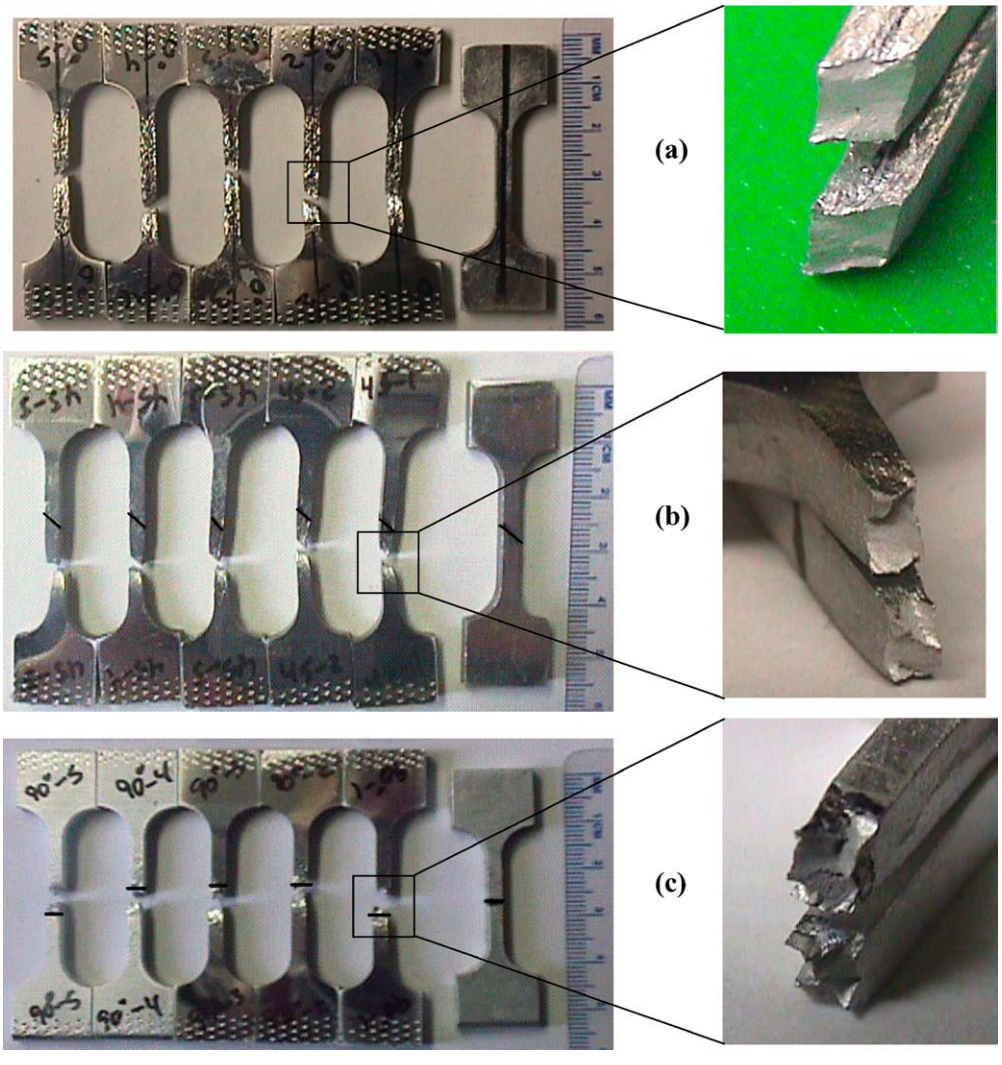

Figure 14 Fractured modes of (a) 0°, (b) 45°, and (c) 90° tensile specimens with weld location marked in relation to fractured plane. On the right is a closer look at typical fracture surfaces.

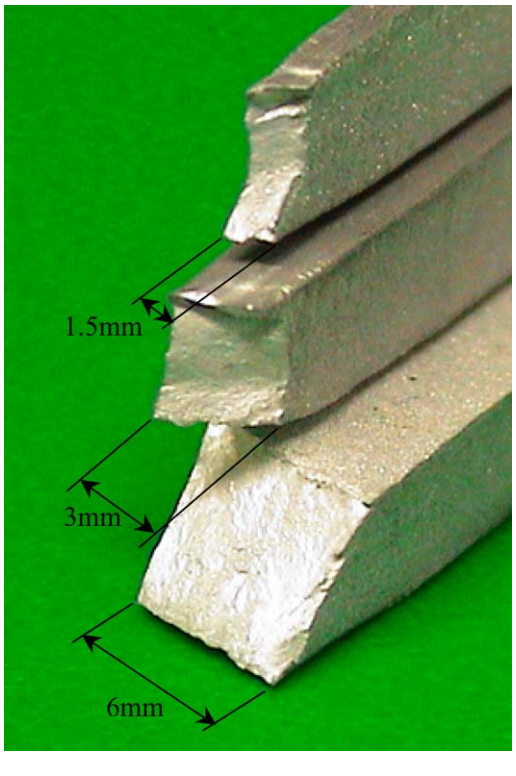

Figure 15 Fracture surfaces of the 0° weld specimens with various widths.

4. Discussion

It was earlier seen in Fig. 9 that the UTS depends mostly on the specimen orientation to the extrusion direction irrespective of the presence of a weld. However, fracture locations, fracture patterns (Fig. 15), and strain to failure (Figs 10 and 13) were significantly affected by the presence of the weld. Therefore, the existence of a weld, its geometry and its microstructure seem to determine the failure characteristics. In the scanning electron micrographs presented in Fig. 6c and d, although precipitates were distributed inside the extrusion weld region and in the parent material, there was a concentration of precipitates that aligned along the charge weld between these two regions. To understand the role of these aligned precipitates on failure characteristics, it is essential to take a closer look at the extrusion process and the conditions under which the extrusion welds are formed. The resulting microstructure within the weld region is also of interest. During the extrusion process, a heated billet is forced into the die cavity, see Fig. 1. As the material flows into the die chamber to form a closed loop cross-section, it must separate around the mandrel supports. These supports must be sufficiently rigid to avoid deflection and movement of the mandrel and to obtain reasonable dimensional tolerances on the final extruded part. As the material flows through the

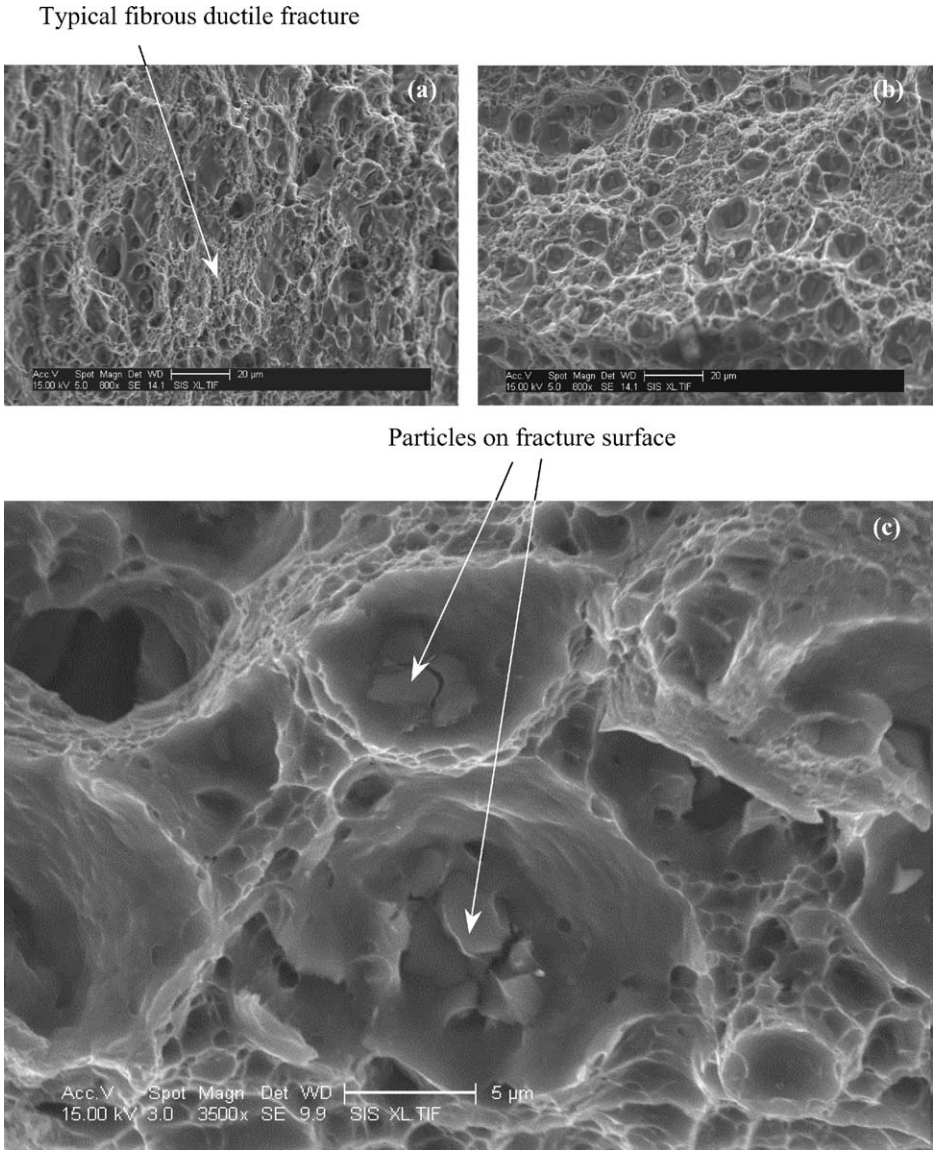

Figure 16 SEM micrographs of the fracture surfaces of specimens with (a) no-weld, (b) 90°-weld, and (c) high magnification micrograph revealing Mg_2Si precipitates.

portholes of the die around the mandrel support, it is subjected to sticking friction and to high shear strains and strain rates. Due to the constraints of the die geometry, the flowing material is subjected to high pressure as it fills the continuously narrowing die cavities after it has separated along the mandrel supports (cross-sectional views A-A and B-B in Fig. 1). During the final stage of the extrusion process (cross-section C-C in Fig. 1c), the separate streams of metal are brought together in a welding chamber where the two shear layers, or interfaces (one on each side of the mandrel support) are welded back together due to high local pressures thus forming a seam weld [3, 6]. The charge weld between the two billets forms as a result of material left behind in the extrusion die, bonding to material from the new billet, as explained earlier. In both welds, there is an "artificial grain boundary" [1], that is formed at the seam weld and charge weld interfaces. These artificial grain boundaries may act as nucleation sites for precipitates in the subsequent strengthening process following the extrusion [7–9].

As the material flows out of the extrusion die in its final shape, it is immediately quenched, creating a supersaturated solid solution. The rate of quenching is carefully controlled to retain a fine dispersion of vacancies, which leads to enhancement of mechanical properties of the material in the subsequent stages of heat treatment. During the aging process, (following the quenching of the extruded material) a fine dispersion of magnesium silicide (Mg_2Si) particles precipitate out of solution. The EDS spectrum (not shown here) taken on the precipitates, shows the presence of magnesium and silicon. Although a fine dispersion of precipitates is desirable for improved material strength, aligned precipitates, shown in Fig. 5c and d may behave similar to rigid inclusions in a matrix leading to failure of the material along this boundary. In the literature, Akeret [1] and Valberg [2] pointed to impurities from improper lubricating and oxides from billet faces that reside on the charge weld interface. In the commercially produced sections received, these issues were alleviated by scrapping the front end of the extrudate. Precipitates and other inter-metallic particles nucleate at these interfacial regions, and play a dominant role in the mechanical behavior of the extrudate. Uni-axial tensile tests performed with the extrusion weld at 90°

to the tensile axis show that the fracture plane is next to this interface. The fracture runs along the interface briefly before shearing through the rest of the material. This would imply that the alignment of the particles shown in Fig. 5 create a "slightly" weaker and less ductile material than the surrounding matrix. These particles on this charge weld interface cause the occurrence of more complex fracture surfaces in the weld region compared to the smooth planar fracture of the no-weld specimens. As discussed in the following, more particles are seen on the fracture surfaces of weld specimens (compared to no-weld specimens) confirming that the stress concentration due to the aligned particles initiates the failure of the material.

To further validate the role of the Mg_2Si particles discussed above on the observed fracture of the charge weld, SEM micrographs on no-weld and 90°-weld specimen fracture (of 1.5 mm width) surfaces are presented in Fig. 16. Careful observation of the micrographs reveals that the 90°-weld fracture surface (Fig. 16b) contains a higher density of voids containing the precipitates than the no-weld specimen fracture surface shown in Fig. 16a. Also note that Fig. 16a reveals more regions of typical ductile fracture compared to the fracture surfaces of the material with weld in Fig. 16b. Fig. 16c shows a high magnification picture of typical void containing the Mg_2Si precipitates. Therefore, it is concluded that the aligned Mg_2Si precipitates are partially, if not primarily, responsible for the observed less ductile behavior of the extrusion weld.

5. Conclusions

Uni-axial tensile tests performed on the specimens with extrusion welds revealed that the extrusion weld influences the fracture location, the failure characteristics and the strain to failure of the extruded material. The UTS and yield strength are moderately affected by the weld and its orientation, but a greater reduction in ductility of the material is noticed when the weld material volume is greatly increased in the specimens. It was seen that failure occurred consistently in the region adjacent to the seam weld, always cutting through the charge weld interface. Microscopic observations in this region revealed a distinct change in grain pattern (Fig. 5b) and precipitation of Mg_2Si particles along the weld/parent material interface. When specimens were tested with a higher volume fraction of weld region, the strain to failure yield strength and UTS decreased significantly indicating more brittle behavior of the weld material. The failure modes were also consistent with this observation. Microscopic observation of failure surfaces revealed that the specimens with an extrusion weld at 45° and 90° have more visible particles than those without an extrusion weld.

Acknowledgement

The authors sincerely acknowledge the support from Hydro Aluminum Technology Center N.A. in Holland, Michigan.

References

1. R. AKERET, in Proceedings of 5th International Aluminum Extrusion Technology Seminar, Chicago (1992) Vol. 1, p. 219.
2. H. VALBERG, *Int. J. Mater. Prod. Tech.* **17**(7) (2002) 497.
3. H. VALBERG, Private Conversation, NTNU, Trondheim, Norway, May 11, 2004.
4. O. GJERSTAD, "Untersuchung der Eigneschaften von Langspressnahten an AlMgSi1-Strangpressprofilen," Thesis (in German), NTNU, Trondheim, Norway, 1999.
5. J. ZASADZINSKI, J. RICHERT and W.MISIOLEK, *Light Metal Age* April (1993) 8.
6. P. K. SAHA, "Aluminum Extrusion Technology" (ASM International, Materials Park, Ohio, 2000).
7. S. STOREN and P. T. MOE, "Extrusion" (Handbook of Aluminum, Physical Metallurgy and Processes) Vol. 1, p. 385.
8. I. J. POLMEAR, "Light Alloys—Metallurgy of the Light Alloys" (Halsted Press, New York, 1995).
9. T. H. COURTNEY, "Mechanical Behavior of Materials" (McGraw-Hill, Boston, 2000).

Received 25 April 2003
and accepted 19 July 2004